Performance Analysis of Mobile IPv6 under Spectrum Mobility in Cognitive Radio (CR) Networks

Manoj Kumar Rana
SMCC
Jadavpur University
Kolkata, India
e-mail: manoj24.rana@gmail.com

Swarup Mandal
Delivery Head
Wipro Limited
Kolkata, India
e-mail: swarup.mandal@wipro.com

Bhaskar Sardar
Dept of IT
Jadavpur University
Kolkata, India
e-mail: bhaskargit@yahoo.co.in

Debashis Saha
MIS Group,
Indian Institute of Management (IIM)
Calcutta, Kolkata, India
e-mail: ds@iimcal.ac.in

Abstract— **In cognitive radio (CR) networks, the secondary users may encounter frequent IP handoffs due to high spectrum mobility, even if they remain static spatially. Since mobile IPv6 (MIPv6) is not originally designed to deal gracefully with such IP handoffs induced by spectrum mobility only, the performance of the IP-based applications running in secondary users (SUs) may degrade severely in such scenarios. This paper conducts a simulation based investigation to gauge the seriousness of the issue and then suggests possible solutions. To do so, we have first developed in ns-3 a CR Attribute Module, and then implemented MIPv6 over it. For SUs, we have considered three spectrum selection strategies, namely Greedy, Most Recently Used, and Least Frequently Used. In each case, we have analyzed how the frequency of IP handoffs varies with the rise in spectrum mobility, resulting in degraded throughput in SUs. Our study reveals that MIPv6 is unable to work properly in CR networks mainly due to the high default values of MIPv6 parameters. So, we propose to customize mobile IPv6 – in terms of appropriating the pre-set values of its parameters – in order to make it work properly in CR networks, especially where the spectrum mobility is high.**

Keywords- Cognitive Radio Network; Spectrum Mobility; Simulation; ns-3; Mobile IPv6 (MIPv6); IP handoff.

I. INTRODUCTION

The ever-increasing popularity of mobile devices and smart phones are causing explosive growth of data traffic in mobile communication networks [1]-[4]. At the same time, the *licensed* spectrum for mobile broadband is becoming limited and hence costly to the mobile operators. However, recent surveys on spectrum occupancy statistics in various countries worldwide reveal that licensed bands are not being utilized fully [3]. This opens up the possibility that a user of a heavily loaded system can harness the underutilized spectrum of another system opportunistically. The well-known approach of dynamic spectrum access employs the cognitive radio (CR) technique, which has been standardized in IEEE 1900.4 [4] and included in the end-to-end efficiency project of the European Telecommunication Standard Institute (ETSI) [5]. According to IEEE 1900.4 [4] and ITU-R M.2330-0 report [6], opportunistic spectrum usage could be another deployment scenario of CR-based dynamic spectrum access in heterogeneous CR networks (CRNs). In CRNs, the base stations/access points (BSs/APs) are assumed to be legacy, operating in a particular radio access technology (RAT), whereas mobile devices, called secondary users (SUs), are reconfigurable terminals (can use different frequency bands of radio access networks (RANs)). Utilization of idle licensed spectrum in this way reduces the capital expenditure as no extra investment is needed for new system installations.

An SU in a CRN switches from one channel to another, when it is interrupted by a licensed device, commonly known as primary user (PU). This event of channel switching is called *spectrum mobility* [7]. Spectrum mobility in a multi-RAT, multi RAN and multi-operator environment causes two types of handoff: *intra-system* handoff and *inter-system* handoff [4]. Switching from a busy channel to a free channel of the same network system at the time of PU arrival causes an intra-system handoff. On the contrary, switching from a busy channel of one network system to a free channel of a different network system at the time of PU arrival is called an inter-system handoff. Inter-system handoff happens typically in a heterogeneous radio environment, where multiple operators use multi-RATs in the same location (for example, Fig. 1). In Fig. 1, one operator has WCDMA commercial network (i.e., a cellular system), while another operator owns IEEE 802.11x technology as a private WLAN system. In such a muti-RAT, multi-operator scenario, inter-system handoff is a major challenge because the conventional handoff management schemes (such as GPRS tunneling protocol used in 3G systems, or, the complex

tunneling mechanism, used in Long Term Evolution (LTE)) used to perform handoff between the same RAT within the same operator's network. Hence, they can be solely based on link layer technology. As a result, these techniques are not suitable for heterogeneous CRNs.

So, there is a strong need to migrate the technology-specific core infrastructure toward all-IP platform, since IP is generic enough to serve all underlying technologies. Although there are numerous IP-based handoff management protocols, we consider mobile IPv6 (MIPv6) [9] in this work because it is the de-facto standard in today's world. As reported by ITU-R [6], the inter-system handoff can be handled through IP layer by implementing a dedicated radio system as the common signaling channel, called basic access network (BAN) [8]. It employs a cognitive pilot channel, standardized in the E3 project, to inform the SUs about the access information, such as the available channels, relevant load and access strategy of each RAT. Due to the dynamic behaviour of radio networks, BANs adopt a handoff strategy that uses the environmental radio information (i.e., channel idleness), useful for opportunistic SUs to switch to the preferred network. The cognitive pilot channel consumes small bandwidth of a licensed/unlicensed channel as reported in [6]. It is used for the sole purpose of signaling only, and not for data transmission.

The focus of our work in this paper is on the performance evaluation of inter-system handoffs caused by spectrum mobility only [10]. We assume that the unavailability of channels in the current network causes an inter-system handoff that ultimately leads to an IP handoff. Thus, eventually, the frequency of IP handoffs depends on the parameters, such as PU arrival rate and PU channel holding time [11]. In CRNs, the number of such IP handoffs may be quite high even when the SU is stationary (i.e., mobility-driven handoffs are practically zero). Moreover, in modern WLAN and LTE or LTE-Advanced (LTE-A) networks, the channel usage occurs in discontinuous mode, i.e., a PU uses a channel for its transmission for a short duration, and then immediately releases the channel for the other PUs [12]. For instance, on an average if a PU has 2^{10} bytes of data to transmit and its transmission rate is 20 Kbps, its average channel holding time is 0.4 s (=(2^{10}*8)/20000). Also, 80% of the spectrum holes in a WLAN are not very big, being only 0-3 s wide [13]. Given such small channel holding times as well as narrow spectrum holes, PU interruption frequency becomes very high. It renders the CRN environment extremely dynamic for the SUs. This, in turn, poses a new set of challenges for the MIPv6 [9] itself because even if the SUs are static, they have to invoke MIPv6 to handle IP handoffs triggered by spectrum mobility.

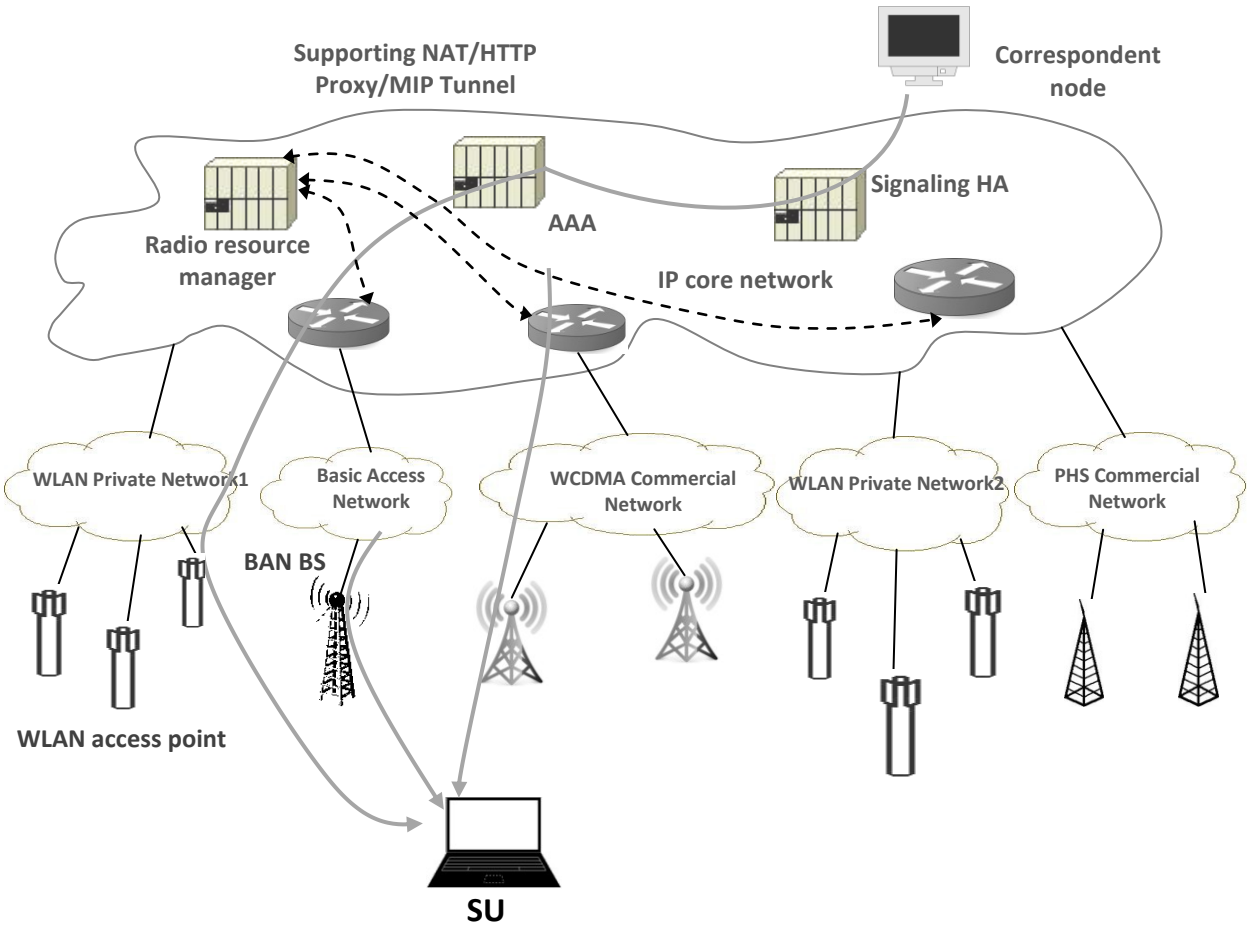

Figure 1. Heterogeneous CR networks: cross-operator handoff with MIP support

MIPv6 was originally designed for handling spatial mobility only, and so it is not optimized for frequent IP handoffs due to inter-system spectrum mobility. It is well known that the handoff procedure in MIPv6 takes a significant amount of time, approximately 1.896 s to 2.47 s [14]. Hence, the net temporal overhead due to multiple IP handoffs may become very high over the complete lifetime of a data connection for an SU, which degrades its data throughput significantly. That is why the objective of this paper is to investigate the performance of MIPv6 in CRNs, in particular, the effect of spectrum mobility on MIPv6. We know that, depending on the movement detection and care-of-address (CoA) configuration strategies, the standard MIPv6 has three flavors: router advertisement (RA) based MIPv6 [9], router solicitation (RS) based MIPv6 [9] and dynamic host configuration protocol (DHCP) based MIPv6 [9][15]. In the first two flavors, an SU uses a stateless address auto-configuration mechanism to configure new CoA. In the third flavor, the DHCP server assigns IP addresses through a dynamic address allocation method [15]. We have performed our analyses using all the three flavors of MIPv6. To simulate a heterogeneous CRN, we have developed the following modules in the network simulator ns-3 [16]: (1) a CR attribute module (CRAM) to mimic a typical CRN, (2) three basic spectrum selection algorithms, namely greedy (GDY), most recently used (MRU), and least frequently used (LFU), and (3) our own MIPv6 module [17] as per RFC 6275 [9].

Our main purpose is to identify exact causes behind the afore-mentioned issues of MIPv6 (in all the three flavors) when used in CRNs. We have investigated the simulation traces and observed that the high values of RA interval, lifetime of CoA, and duplicate address detection (DAD) timers are primarily responsible for the poor performance of MIPv6. Next, we have validated the numerical results with our simulation results. Finally, we have suggested the suitable values for CoA lifetime and DAD period for possible use in heterogeneous CRNs. Also, we have measured the throughput performance of SUs for different spectrum selection algorithms, by varying the PU arrival rate and PU channel holding time. It is worth mentioning here that this paper is an extended version of [1] to report additional numerical analyses, wide-ranging simulation results, new validation exercises, and explanatory notes.

The rest of the paper is organized as follows. In Section II, we discuss recent research works on spectrum handoff and IP handoff in CRNs. Section III provides a brief description of our model implementations in ns-3. Section IV illustrates the MIPv6 issues noted in the considered heterogeneous CRNs. In Section V, we have analyzed the number of IP handoffs and its impact on throughput of the SUs. Finally, Section VI recommends the suitable modifications needed to overcome the issues with MIPv6.

II. Related Works

To access the Internet services using CRNs, the SUs cycle through three sequential phases: *spectrum handoff* phase, *IP handoff* phase, and *data transmission* phase. The spectrum handoff phase consists of channel sensing, handoff decision, pause, and channel switching functions [7]. Similarly, IP handoff phase consists of RA, CoA formation, and tunnel setup [9]. The phase transition is illustrated in Fig. 2. During data transmission, if reappearance of PU occurs, then the SU moves again to channel sensing phase, where the SU attempts to find spectrum holes to switch to. If an empty channel is unavailable, the SU continues sensing the set of busy channels, repeating channel sensing and pause phases continuously. In the spectrum decision phase, the SU decides the best channel to switch to, among the available channels. The selection logic is closely related to the channel characteristics, and the operations of the PUs and the SUs. In the channel switch phase, the SU changes its operating channel. If the channel switch occurs in the same system, data transmission resumes immediately; otherwise, the SU encounters an additional IP handoff.

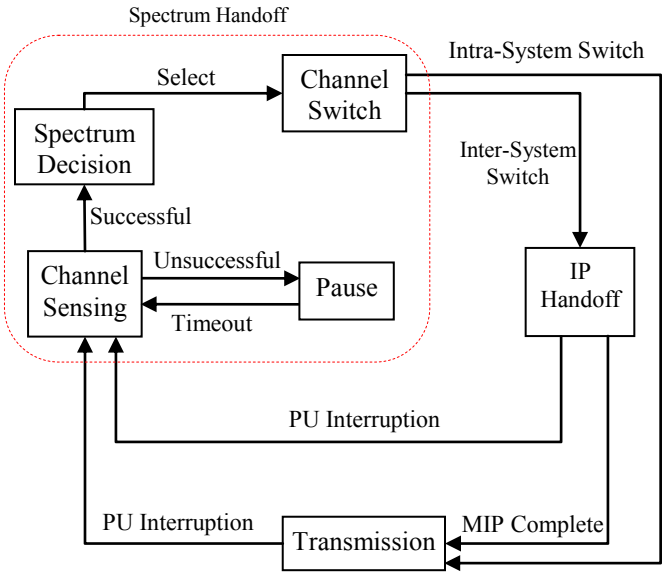

Figure 2. Mobility phase diagram in CRNs

Though many recent research works focus on spectrum mobility in CRNs, only a few of those focus on the resulting IP handoffs and problems thereof faced by SUs. Some of the previous works try to reduce MIPv6 handoff delay in heterogeneous CRNs, through integrated system architecture [10] and using a cross-layer protocol [11].

A. Spectrum Handoff

Wang et al. [18][19] have proposed a dynamic programming based greedy algorithm to determine the optimal target channel sequence, and proved that the greedy algorithm provides the same results as the dynamic programming based algorithm, but with lower time complexity. To optimize the data delivery time, a traffic-adaptive spectrum handoff mechanism is proposed in [19]. It changes the target channel sequence of spectrum handoffs based on traffic conditions. Southwell et al. [20] analyzed spectrum handoff delay, considering the cost of channel switching and congestion due to multiple SUs, with prior knowledge of heterogeneous channels. They have proposed a fast algorithm to determine the best single-user decision,

depending on other user's plans without communicating with each other.

B. IP Handoff

In [10], Kataoka et al. have proposed an MIP-based CRN architecture to reduce the handoff delay. The system architecture contains a control node that integrates multi-RAT access points and a unified authentication, authorization and accounting (AAA) server that performs authentication, authorization and charging on behalf of all networks. The AAA server provides a single IP address to SUs while roaming among multiple networks and a control node manages the IP handoff through a fast routing based scheme. However, the downside of this protocol is that the control node becomes a bottleneck and this may result in a single point failure. Chen et al. [11] have proposed a cross-layer protocol to optimize the data transmission time in CR LTE networks. Since the authors have assumed homogeneous LTE networks, they have not used MIPv6. Instead they have used the standard LTE handoff mechanism which takes only a few ms; so there is not much impact of IP handoff on transmission time.

The above existing proposals have been made to reduce the IP handoff latency in CRNs. They are unable to report thus far the issues of network layer mobility management protocols, such as MIPv6 in CRNs. Also, no prior works exist to show the impact of spectrum mobility alone on MIPv6. These observations call for a detailed analysis of MIPv6 in heterogeneous CRNs, which may give us an insight into the practical design issues of MIPv6 and the impact of spectrum mobility on IP handoffs.

III. COGNITIVE RADIO ATTRIBUTE MODEL (CRAM)

We have implemented CRAM in ns-3 [16]. It takes traffic parameters and spectrum selection strategy as input. We describe CRAM in the following three subsections.

A. Traffic Parameters

We consider *network1* with *C1* number of channels and *network2* with *C2* number of channels. At any point in time, each of these channels can be occupied by a PU or an SU or remains empty. We have assumed that *network2* has higher preference over *network1* for SUs, i.e., an SU switches to *network1* if and only if *network2* is unavailable. For simplicity, we have assumed homogeneous traffic parameters for all channels and the PU traffic parameters are same for *network1* and *network2*. We have assumed that the PU and SU arrival processes follow a Poisson distribution while their service times follow an exponential distribution. Table I lists the variables used in this section.

Using Little's formula, we can write

$$\rho_p = \lambda_p E[X_p] \quad (1)$$

$$\rho_{s,1} = \lambda_{s,1} E[X_s] \quad (2)$$

$$\rho_{s,2} = \lambda_{s,2} E[X_s] \quad (3)$$

To calculate the arrival rate for SUs for both the networks, we use the state transition diagram shown in Fig. 3

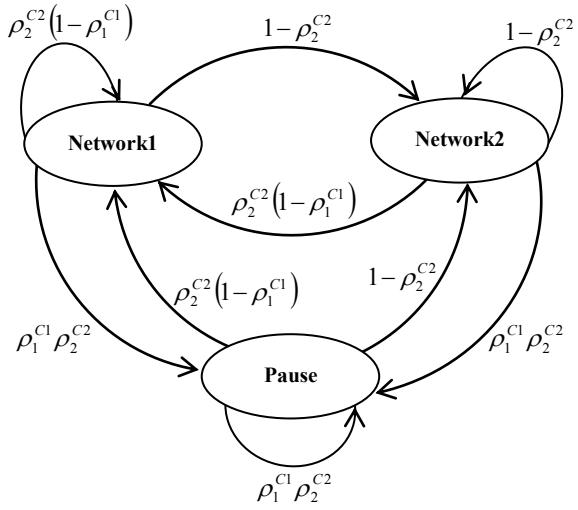

Figure 3. State transition diagram of network switching by SUs

that depicts the probabilities of network switching as a function of ρ_1 and ρ_2. The SU enters *network2* if there exists at least one empty channel and enters *network1* if all the channels of *network2* are busy and at least one empty channel is available in *network1*. So, $\lambda_{s,1}$ and $\lambda_{s,2}$ can be computed as follows:

$$\lambda_{s,1} = \left(1-\rho_1^{C1}\right)\rho_2^{C2}\lambda_s \quad (4)$$

$$\lambda_{s,2} = \left(1-\rho_2^{C2}\right)\lambda_s \quad (5)$$

TABLE I. TRAFFIC PARAMETERS

Parameters	Meaning
$C1$	Number of channels in network1
$C2$	Number of channels in network2
λ_p	PU arrival rate
λ_s	SU arrival rate
$\lambda_{s,1}$	SU arrival rate in network1
$\lambda_{s,2}$	SU arrival rate in network2
X_p	Service time for PUs
$E[X_p]$	Average service time for PUs
μ_p	Average expected Service rate of PUs with mean $1/E[X_p]$
μ_s	Average expected Service rate of SUs with mean $1/E[X_s]$
X_s	Service time for SUs
$E[X_s]$	Average service time for SUs
ρ_p	Channel busy probability or utilization factor by PUs
ρ_s	Channel utilization factor or channel busy probability by SUs, if it is served by network2 only
ρ_1	Overall channel utilization factors or channel busy probability by PUs in network1
ρ_2	Overall channel utilization factors or, channel busy probability by SUs in network2
$\rho_{s,1}$	Channel busy probabilities by SUs in network1
$\rho_{s,2}$	Channel busy probabilities by SUs in network2
$E[N_S]$	Average number of SUs
I_p	Inter-arrival time of the PUs
W	Spectrum hole duration

Now, $\rho_s = \lambda_s E[X_s]$, is the channel utilization factor for the SU, if it is served by *network2* only. Using the values of $\lambda_{s,1}$ and $\lambda_{s,2}$ (obtained using (4) and (5)), from (2) and (3) we get the following equations:

$$\rho_{s,1} = \left(1 - \rho_1^{C1}\right)\rho_2^{C2}\rho_s \quad (6)$$

$$\rho_{s,2} = \left(1 - \rho_2^{C2}\right)\rho_s \quad (7)$$

Hence, the overall channel utilization for *network1* and *network2* are calculated as:

$$\rho_1 = \rho_p + \rho_{s,1} \quad (8)$$

$$\rho_2 = \rho_p + \rho_{s,2} \quad (9)$$

To obtain ρ_s, we use M/M/C queuing model, where C denotes the number of channels being used to serve the SUs. From the definition of M/M/C queue, the average number of SUs in the system can be written as [21]:

$$E[N_S] = C\rho_s + \frac{\rho_s}{1-\rho_s} D\left(C, \frac{\lambda_s}{\mu_s}\right) \quad (10)$$

where

$$D\left(C, \frac{\lambda_s}{\mu_s}\right) = \frac{\frac{(C\rho_S)^C}{C!}\frac{1}{1-\rho_S}}{\sum_{k=0}^{C-1}\frac{(C\rho_S)^k}{k!} + \frac{(C\rho_S)^C}{C!}\frac{1}{1-\rho_S}} \quad (11)$$

which is Erlang's C formula. Using the above formula, we can compute ρ_s, taking $E[N_s]$ as input and replacing C by $C2$. Using (6), (7), (8) and (9), we can numerically solve for ρ_1 and ρ_2.

It is to be noted that the PU inter-arrival time is memory-less and follows exponential distribution with rate λ_p. The distribution of W is the difference of the distributions of I_p and X_p. So the probability mass function of W can be given as follows:

$$f(W=t) = \int_0^\infty P(I_p = x+t)P(X_p = x)dx = \frac{\lambda_p\mu_p}{\lambda_p+\mu_p} e^{-t\lambda_p} \quad (12)$$

B. Spectrum Selection Strategies

We have implemented three spectrum selection strategies: GDY [18][22], MRU [23], and LFU [24]. These strategies are implemented based on the statistical information of the channels. In GDY strategy, the SU selects the first empty channel without any pre-estimation of its freeness. The works in [18] and [22] on modeling and analysis of spectrum mobility events assumed GDY strategy (called first-come-first-served in their system model). The GDY strategy is an opportunistic one; it selects the first empty channel, not targeting to utilize the spectrum holes optimally [18]. In contrast, several other research works [10][23][24] adopt selection strategies to utilize spectrum holes efficiently for the purpose of load balancing among channels as well as reducing data transmission time and improving throughput of SUs. These works consider the typical heterogeneous CRN environment [10] with multiple PUs and SUs [18][23][24]. We also assume this type of scenario in this work. The MRU and LFU are selected as two efficient spectrum selection strategies based on the concepts applied in [23] and [24], respectively. In the MRU strategy, the SU selects the channel which has been used most recently by a PU, expecting a lengthy absence of PUs in that channel in the near future. In LFU strategy, the SU selects the channel which has been least used by the PUs thus far, hoping that it will remain so in the near future too. We have assumed the arrival process of PUs follow Poisson distribution. The GDY strategy selects an idle channel randomly, not considering the available spectrum hole duration. On the other hand, the LFU strategy enhances the utilization rate of a low utilized channel. But, accessing the channel which has been used by a PU most recently, would give the high chance of getting longest spectrum hole due to the Poisson arrival of PUs. In this regard, MRU always selects the longer spectrum hole than the other two strategies.

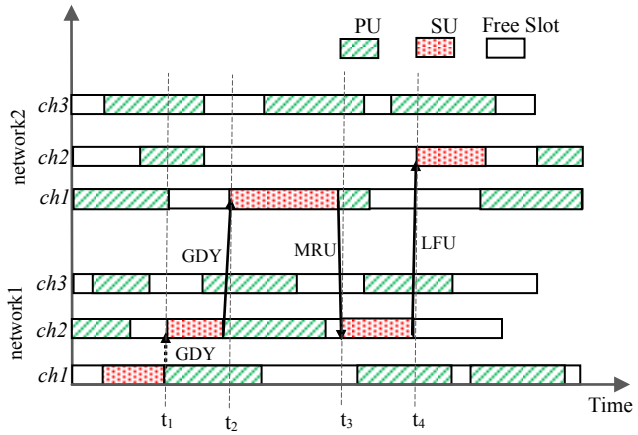

Figure 4. Spectrum mobility in CRNs

In Fig. 4, we have illustrated spectrum selection by a SU using these three strategies. At the time t_1 and t_2, the SU follows the GDY strategy to switch channel. At time t_1, the SU selects the spectrum hole of the first channel of *network1* even though channel 3 is also empty. Similarly, at time t_2, the SU selects the spectrum hole of the first channel of *network2*. At time t_3, the SU follows MRU strategy and selects the spectrum hole of channel 2 of *network1* as it is used most currently among the empty channels. At time t_4, the SU uses LFU strategy to switch to channel 2 of *network2* as the usage percentage of the channel by PU is less than other free channels.

C. CRAM Implementation in ns-3

We used the Time, Timer, Simulator, and RandomVariable classes to implement CRAM. The Time

and Timer classes are used to schedule a task, such as assigning a channel to a SU/PU for a particular time interval and cancel it after completion of the task. The Simulator class is used for initial scheduling of the entire task in the simulation, i.e., it starts the PU and SU transmissions. The RandomVariable class is used to generate exponentially distributed random numbers. We used two schedulers: channel scheduler (Fig. 5) and SU scheduler (Fig. 6). The channel scheduler takes the mean value of λ_p and X_p as input. Following the distribution, the sequence generator generates a large number of sequences (over 1000). Each sequence consists of PU service time and duration of spectrum holes. During simulation, it makes the state of the channel either busy or free, based on the generated values. In the PU busy state, the channel scheduler starts the PU timer and makes the state as busy. After expiration of the PU timer, the free timer starts and the channel state becomes free. It would remain free up to the spectrum hole duration of the current sequence unless an SU sends a busy trigger. The SU busy trigger changes the channel state into busy state such that all SUs see that channel as busy. But, PU can interrupt the SU at any time and the SU has to move to another free channel or, pause state, if there is no free channel available. After expiration, it queries for the next sequence. A channel sensor database is implemented that acquires the channel information.

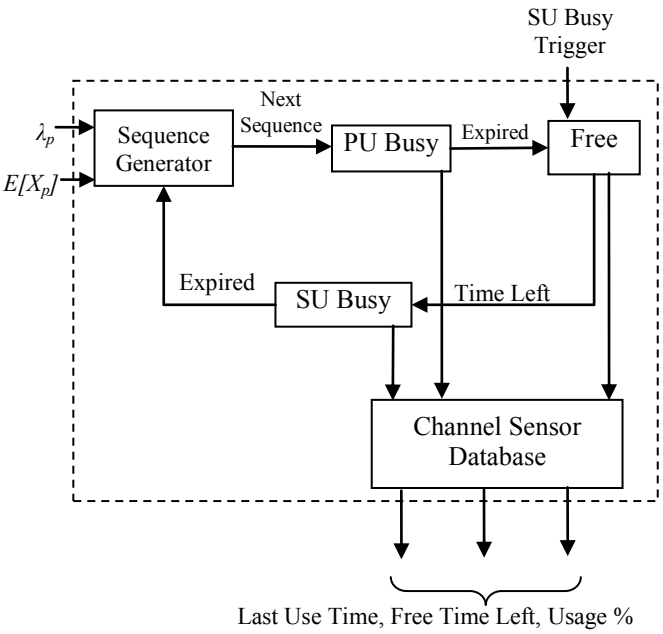

Figure 5. CRAM Channel Scheduler

In the SU scheduler, the user inputs its data transmission time and the spectrum selection strategy. The spectrum selection strategy acquires the channel information from all channels of all systems and makes a decision. It outputs the next channel number (k) and the remaining free time. If it gets the free time slot, it starts a transmission timer, giving a busy trigger to the k^{th} channel scheduler. The start

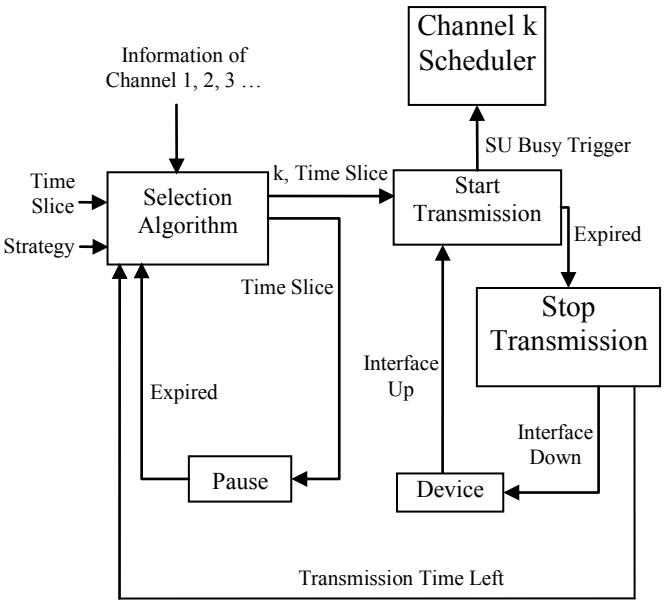

Figure 6. CRAM SU Scheduler

transmission functionality makes the SU's *network1* or, *network2* netdevice state into 'UP'. The Stop Transmission function makes the SU's corresponding state into 'Down' state. If at any point in time, the spectrum selection strategy cannot find a free channel, it pauses for a predefined timer value. After expiration of the pause timer, it again runs the spectrum selection strategy.

IV. MIPv6 ISSUES IN CRNS

We have developed our own MIPv6 module [17] for ns-3 (as it is not available currently) on top of CRAM.

A. Simulation setup

We have considered two networks: *network1* and *network2* containing 20 and 10 channels respectively. The SU is opportunistic to *network2*. We used a constant position mobility model for the SUs because we are not interested in spatial mobility. We used λ_p = 1.5 and $E[N_s]$ = 4. Since multiple SUs are used, the contention among the SUs to access the same spectrum hole is managed through periodic sensing as shown in Fig. 2. It is to be noted that, for simplicity, we have measured the throughput performance of single SU. We used exponentially distributed connections with average connection length 480 bytes [25]. So, when the data rate of primary connection is 19.2 Kbps [25], we have $E[X_p]$= (480*8)/(19.2*10^3)=0.2 s. The Pause timeout value and spectrum handoff delay are set as 0.05 s and 0.01 s, respectively. The correspondent node (CN) and SU are running '*UDP Echo*' application and transferring packets at the rate of 80 Kbps. In this simulation, we keep the data rate fixed for all the PUs and the SUs. The whole simulation is run for 1000 s. However, we present only the results selected from 100 s. to 200 s. to highlight the design issues.

B. High RA Interval and Lifetime Period

1) Problem Description

If the duration of spectrum holes is very small, an SU may switch from one network (say *network2*) to another (say *network1*), reside there for a very short time, and then may return to *network2* again. When the SU switches to *network1*, the address configured in *network2* still remains valid for some more time. If it returns to *network2* quickly, it could use the previously configured CoA in *network2*, giving rise to two issues. *First*, when the SU is in *network1*, another SU in *network2* may configure the same CoA and execute DAD procedure. The DAD procedure detects the address as valid for obvious reasons. So, when the SU returns to *network2* quickly, duplicate addresses would exist in *network2* even if the DAD procedure detects no duplicity. So, the SU will use duplicate CoA in CRN if it makes a quick return in the old network. *Second*, the binding update and tunnel setup procedures in MIPv6 are always triggered after the completion of the DAD procedure. So, if the SU uses a previously configured CoA in *network2*, those procedures are skipped. Since MIPv6 is not triggered, the tunnel set up between the SU and its home agent (HA) would still be the older one and the traffic would not be redirected towards the SU. As a result, the performance of the SU degrades drastically.

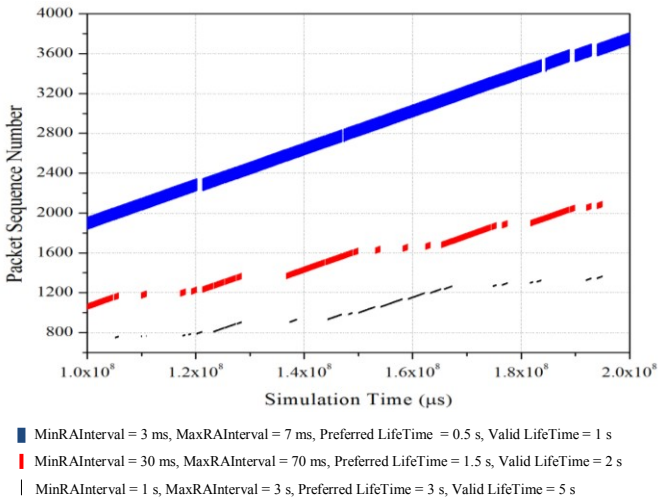

Figure 7. Behaviour under High RA and lifetime period in case of RA-based MIPv6

To illustrate the problem we have performed simulations for the RA-based and RS-based MIPv6 cases, but not for DHCP-based MIPv6, because DHCP eliminates the DAD period, and thus, does not suffer from this problem. In Fig. 7, we illustrate the impact of high RA interval and lifetime duration on packet flow in CRNs for RA-based MIPv6. First, we used MaxRAInterval=3 s and MinRAInterval=1 s as given in [14]. So, after switching back to *network1*, the SU does not perform MIPv6 operations for a long time due to high RA interval and lifetime period. This is evident from long gaps in packet sequence number in Fig. 7. Next, we decreased the values of the RA interval to MaxRAInterval=0.07 s and MinRAInterval=0.03 s. The corresponding simulation result (Fig. 7) shows that MIPv6 is unable to work gracefully, resulting in long gaps in packet sequence number. So, we further reduced the values of RA intervals to 7ms (MaxRAInterval) and 3ms (MinRAInterval), and then we found that all MIPv6 operations are completed successfully (Fig. 7). We also observed that, under this circumstance, a large number of control packets are being generated, leading to congestion. So, we argue that the *RA interval and lifetime period must be set considerably low in order to be appropriate for use in CRNs*.

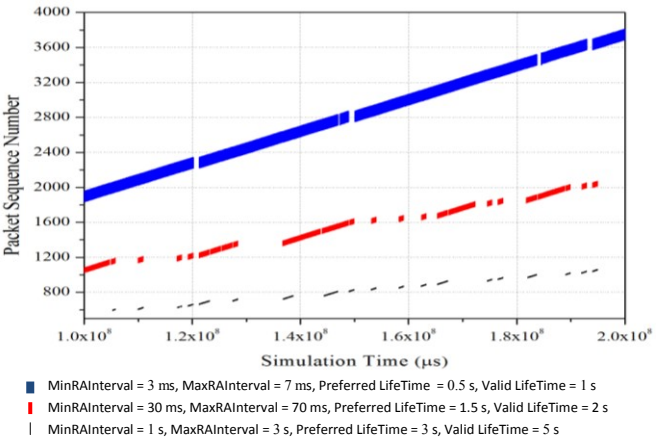

Figure 8. Behaviour under High RA and lifetime period in case of RS-based MIPv6

In Fig. 8, we illustrate that problem for RS-based MIPv6, taking the same set of values of RA interval and lifetime period. In this case, RS is sent by an SU after the link layer attachment and access point returns RA in response to RS. So, the RA delay is reduced but not completely eliminated. In this case, the SU receives RA more quickly than in the previous case. But, since the previously configured address still remains valid, the problem becomes more severe than RA-based MIPv6. The difference is seen in case of RA interval between 1-3 s. Comparing Figs. 7 and 8, we observe that there are more gaps in packet sequence number in RS-based MIPv6 than that in RA-based MIPv6. So, RS-based MIPv6, which actually reduces handoff delay, degrades performance much more than RA-based MIPv6 does. However, this difference is not seen in cases of small RA intervals like 30-70 ms and 3-7 ms, as the RA interval and RS delay are almost the same in these cases.

TABLE II. MIPV6 HANDOFF PARAMETERS

Parameter	Meaning	Parameter	Meaning
R_M	Max RA Interval	R_m	Min RA Interval
R_A	RA Delay	T_{VL}	IPv6 Address Valid Lifetime
T_{DHCP}	DHCP address acquisition delay	R_S	RS Delay
τ	Wireless hop delay	T_{BU}	BU Delay
T_{DAD}	DAD period	T_{SH}	Spectrum handoff delay
T_L	Link layer attachment delay		

2) Validation with the Numerical Results

To validate the '*MIPv6 not triggered*' problem, we use the MIPv6 handoff parameters given in Table II. The timing diagram, shown in Fig. 9, presents the timing of RA message reception by the SU and the behavior of address expiry timer in case of RA-based MIPv6. After getting RA in *network2*, the SU switches to *network1* following a spectrum handoff and returns back to *network2* that provides the RA message again. The address expiry timer is last updated when the SU receives the RA message before switching to *network1*, as indicated in Fig. 9. After switching back to network2, the old address, previously configured in network2, is not expired and the SU uses that address without configuring a new address Hence, DAD is not performed and MIPv6 is not triggered. After getting RA in *network2* again, the life time timer will be updated again. So, the total time elapsed between these two updates is $2R_A + \frac{W}{2} + 2T_{SH}$. Here, we assume the spectrum hole duration as *W/2*, instead of *W*, because the SU acquires the spectrum hole randomly in between *0* to *W* interval. The '*MIPv6 not triggered*' problem happens if the valid lifetime is greater than the elapsed time between two updates in *network2*. So, the probability of the problem can be calculated as follows:

$$T_{VL} > 2R_A + \frac{W}{2} + 2T_{SH} = P(W < 2(T_{VL} - 2R_A - 2T_{SH})) \quad (13)$$

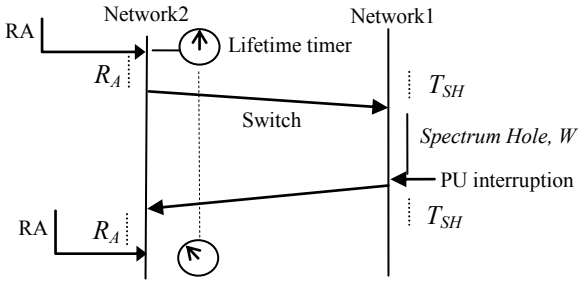

Figure 9. Timing diagram for RA-based MIPv6

In the previous case, if the SU continues in *network1*, even after PU interrupt, due to channel unavailability in *network2*, then the stay time in *network1* will increase. For two such PU interruptions, the spectrum hole value would be *2*W/2*. So if the SU returns to *network2* after '*n*' PU interrupts in *network1*, then the probability of '*MIPv6 not triggered*' problem would be:

$$\begin{aligned} & P\left(T_{VL} > 2R_A + n * \frac{W}{2} + (n+1)T_{SH} \right) \\ & = P\left(W < (\frac{2}{n}) * (T_{VL} - 2R_A - (n+1)T_{SH}) \right) \\ & = P\left(W < \frac{L}{n} \right) \end{aligned} \quad (14)$$

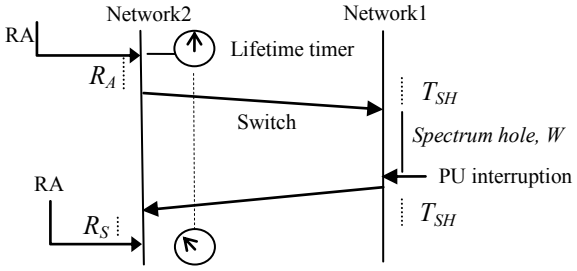

Figure 10. Timing diagram for RS-based MIPv6

where $L = 2\left(T_{VL} - 2R_A - (n+1)T_{SH}\right)$ is a constant. Using the state transition diagram, shown in Fig. 3, the total probability of '*MIPv6 not triggered*' problem can be calculated as follows:

$$\begin{aligned} P\left(MIPv6\_Not\_Triggered\right) = & \sum_{n=1}^{\infty} f(W < \frac{L}{n}) * \\ & \left(\rho_2^{C2}\left(1-\rho_1^{C1}\right)\right)^{n-1} * \left(1-\rho_2^{C2}\right) \end{aligned} \quad (15)$$

where $f\left(W < (\frac{2}{n}) * L\right)$ can be calculated from (12) as follows:

$$\begin{aligned} f\left(W < \frac{L}{n}\right) &= \int_0^{\frac{L}{n}} f\left(W = t\right) \\ &= \int_0^{\frac{L}{n}} \frac{\lambda_p \mu_p}{\lambda_p + \mu_p} e^{-t\lambda_p} dt \\ &= \frac{\mu_p}{\lambda_p + \mu_p}\left(1 - e^{-(\frac{L}{n})\lambda_p}\right) \end{aligned} \quad (16)$$

It is to be noted that the RA delay depends upon the RA intervals set by the AR and the attachment timing of the SU to the new link. As given in [26], R_A can be given as follows:

$$R_A = \frac{R_M^2 + R_M R_m + R_m^2}{3\left(R_M + R_m\right)} \quad (17)$$

The timing diagram for RS-based MIPv6 is shown in Fig. 10. The SU receives RA quickly after switching to *network2*. The probability of '*MIPv6 not triggered"* problem, if the SU returns to *network2* after '*n*' PU interrupts in *network1*, would be as follows:

$$P\left(T_{VL} > R_A + R_S + n*\frac{W}{2} + (n+1)T_{SH}\right) = P\left(W < (\frac{2}{n})*(T_{VL} - R_A - R_S - (n+1)T_{SH})\right) \quad (18)$$

It is to be noted that the RS delay is two times the wireless hop delay, i.e., $R_S=2*\tau$. The total probability of '*MIPv6 not triggered*' problem can be computed in the similar way as in (15).

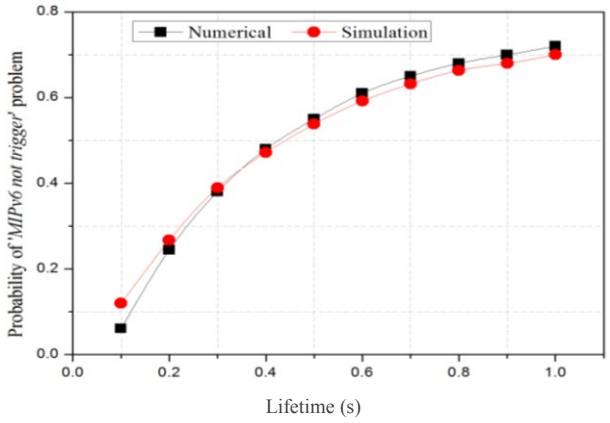

Figure 11. Validation graph for "MIPv6 not triggered" problem in RA-based MIPv6

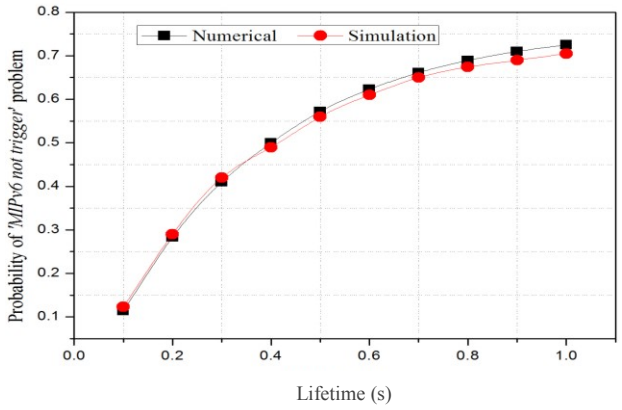

Figure 12. Validation graph for "MIPv6 not triggered" problem in RS-based MIPv6

The validation graphs for RA-based and RS-based MIPv6 are shown in Fig. 11 and Fig. 12, respectively. Taking τ=0.1 ms, R_m=30 ms, and R_M=70 ms, we vary T_{VL} to obtain the total probability of occurrence of '*MIPv6 not triggered*' problem. In our simulation, we find this probability by counting occurrences of the problem and dividing it by the total number of switches from *network1* to *network2*. It is to be noted that the chance of occurrence of the problem will increase if W in *network1* is less than T_{VL} in *network2*. The time of stay of SU in *network1* mainly depends on W, which is an exponential variable with mean 0.52 s, computed using (12). So, if T_{VL} is increased from 0 to the mean of W, there is a sharp increase in the probability due to the increase in the number of spectrum holes. For T_{VL}=0.52 s to T_{VL}=1.0 s, there are fewer cases where W lies between mean of W and T_{VL}. First, the frequency of spectrum holes decreases after the mean due to its exponential property. Second, the stay time of SU in *network1* depends on the number of PU interruptions and the probability of high PU interruptions is small, as indicated in (15). So, the rate of increase in probability is slow in this period. It is to be noted that, in both graphs, the numerical results almost match with the simulation results, which validates our simulation work.

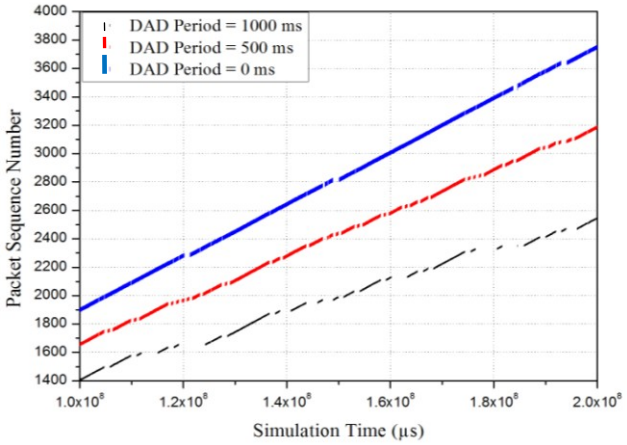

Figure 13. Behaviour of RA-based MIPv6 under High DAD period

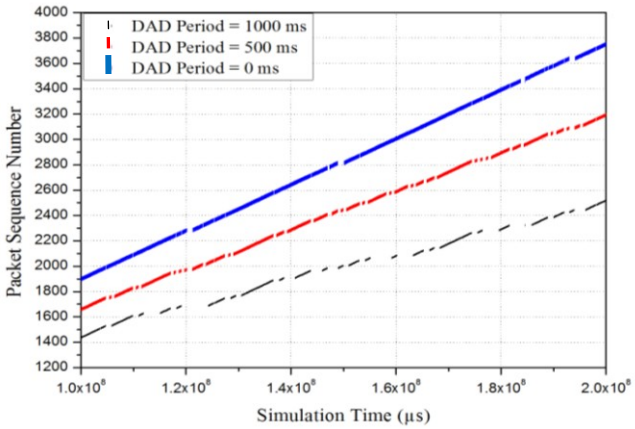

Figure 14. Behaviour of RS-based MIPv6 under High DAD period

C. *High DAD Period*

1) *Problem Description*

RFC 6275 [9] has mentioned the default DAD period as 1 s, which may be higher than the considered duration of spectrum holes in CRNs. Whenever an SU switches to a new network, the address configuration procedure – in particular, the DAD procedure – consumes almost the entire spectrum hole, and hence, the spectrum hole cannot be used for data

transmission at all (Fig. 13 and Fig. 14). So, the throughput of SUs degrades in CRNs. For this reason, the DAD period must also be reduced to make MIPv6 more effective in CRNs.

2) Validation with the Numerical Results

The RA-based MIPv6 handoff delay can be given as follows,

$$T_{HO} = T_L + R_A + T_{DAD} + T_{BU} \quad (19)$$

For the successful completion of the MIPv6 handoff process, the handoff delay must be less than the spectrum hole value. So the '*incomplete IP handoff*' problem for one PU interruption happens if the condition, $W/2 < T_L+R_A+T_{DAD}+T_{BU}$ holds. For 'n' PU interruptions, the probability of occurrence of '*incomplete IP handoff*' problem would be:

$$P\left((n/2)*W < T_{HO}\right) = P\left(W < (2/n)*T_{HO}\right) \quad (20)$$

Assuming, $S=2*T_{HO}$, we can compute the total probability of '*incomplete IP handoff*' problem using (15), by replacing L by S. In case of RS-based MIPv6, R_A is to be replaced by R_S in (19). The total probability can be computed in the similar way as given in (15).

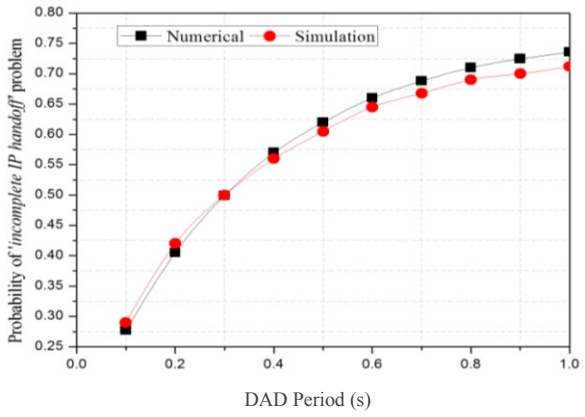

Figure 15. Validation graph for "incomplete IP handoff" problem in RA-based MIPv6

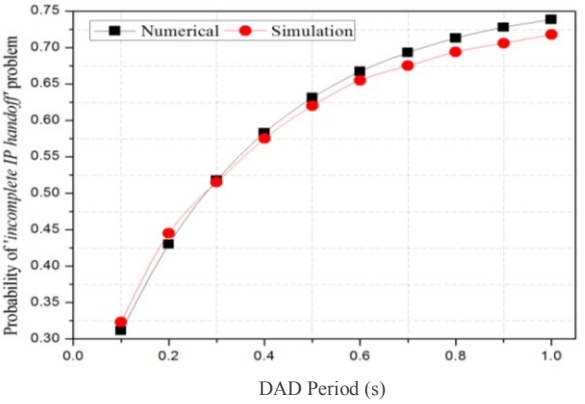

Figure 16. Validation graph for "incomplete IP handoff" problem in RS-based MIPv6

The validation graphs for '*incomplete IP handoff*' problem are shown in Fig. 15 and Fig. 16 in the case of RA-based and RS-based MIPv6, respectively. Taking T_L=10 ms and T_{BU}=23 ms, we vary T_{DAD} to obtain the total probability of occurrence of '*incomplete IP handoff*' problem in *network1*. The '*incomplete IP handoff*' problem occurs if the IP handoff delay is higher than the spectrum hole duration. It is known that T_{DAD} is the dominant delay component in the IP handoff delay. So, the chance of the problem will increase if we increase T_{DAD}. We observed that the frequency of W in *network1* is high but with small spectrum hole durations for T_{DAD}=0 to T_{DAD}=0.52 s. due to its exponential nature. So, with increase in T_{DAD} from 0 to 0.52 s, the probability of occurrence of the problem increases sharply. Also due to the exponential nature of W, for T_{DAD}= 0.52 s to T_{DAD}=1.0 s, the frequency of W is reduced with small spectrum hole duration. So, the rate of increase in the probability is slow in this period. It is to be noted that the numerical results nearly match with the simulation results, thereby validating the correctness of our simulation.

TABLE III. SIMULATION PARAMETER VALUES

Variable Parameter	Other Parameter Values
λ_p	$(E[X_P])_{LOW}$=0.1, $(E[X_P])_{HIGH}$=0.3, $E[N_S]$=4
$E[X_p]$	$(\lambda_p)_{LOW}$=1, $(\lambda_p)_{HIGH}$=1.5, $E[N_S]$=4
$E[N_S]$	$(\lambda_p)_{LOW}$=2.0, $(\lambda_p)_{HIGH}$=2.5, $(E[X_P])_{LOW}$=0.1, $(E[X_P])_{HIGH}$=0.3

V. ANALYSIS OF THE IMPACT OF SPECTRUM MOBILITY

In this section, we present the main results and discuss their implications at length. Here, we have made some minor changes in the simulation setup used in Section IV-A, in order to bring in more randomness in the availability of spectrum holes. The channels of CRAM are characterized as either of high usage or of low usage, to benefit from LFU and MRU strategies. We have used λ_p, $E[X_p]$, and $E[N_s]$ variables to control the emptiness of the channels (Table III). Also, to alleviate the problems explained in Section IV, we have taken 7 ms and 3 ms for MaxRAInterval and MinRAInterval, respectively. The preferred lifetime values are assumed to be 0.5 s and 1 s, respectively. The simulation has been performed for RA-based and DHCP-based MIPv6 only, and not for RS-based MIPv6. This is because, for small RA intervals, RS-based MIPv6 behaves almost similarly as RA-based MIPv6 does.

We have randomly assigned either $E[X_p]_{HIGH}$ or $E[X_p]_{LOW}$ values in all 30 channels, while keeping $E[N_s]$=4. Increasing λ_p increases the frequency of spectrum holes but with reduced duration of each. From Fig. 17, we observe that, up to $\lambda_p \leq 2.8$, the number of IP handoffs increases sub-linearly, and, for $\lambda_p > 2.8$, the frequency drops abruptly. So PU arrival rate of 3 per s acts as a kind of threshold for this experimental setting. We note that, for $0.1 \leq \lambda_p \leq 2.2$, all IP handoffs are completed successfully due to sufficiently large spans of the spectrum holes. As a result, the throughput of the SU is reduced only slightly (this reduction is primarily due to the lengthy handoff operation of MIPv6) as shown in

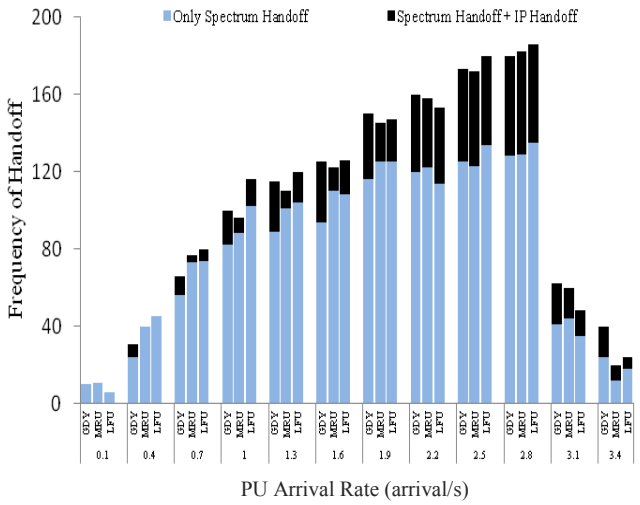

Figure 17. Variation of IP handoff with PU arrival rate

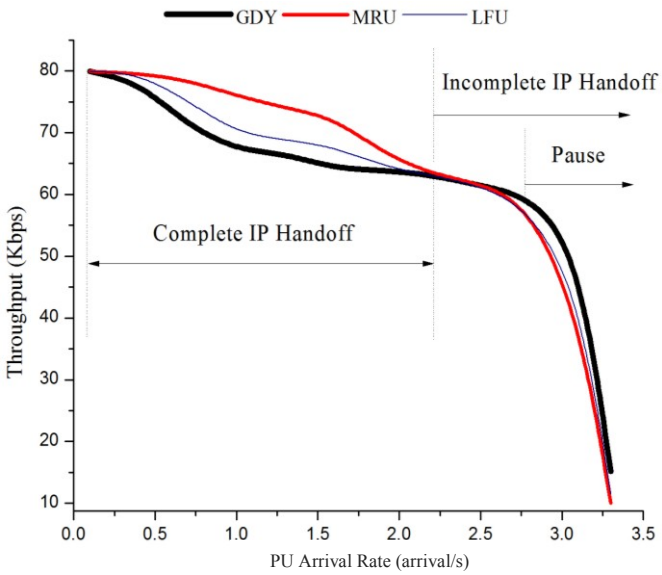

Figure 18. Effect of PU arrival rate on throughput of SU in case of RA-based MIPv6

Fig. 18. For $2.2<\lambda_p\leq2.8$, some spectrum holes become squeezed resulting in few incomplete IP handoffs. However, the number of incomplete handoffs is not significant enough to cause drastic degradation in the throughput of the SUs (Fig. 18). But, when $\lambda_p>2.8$, the spectrum holes become really small to allow almost any handoff to be finished in such a short duration. So, the SUs do not get the opportunity to complete spectrum handoff as well as IP handoff most of the time. In this case, the SUs cycle between pause and channel sensing phases (Fig. 2), thereby reducing the throughput of the SUs drastically (Fig. 18). However, in the case of DHCP-based MIPv6, incomplete IP handoff does not occur at all because DAD process is not used; as a result, there is no sharp degradation of throughput initially (Fig. 19). But, beyond $\lambda_p=2.2$, the holes become too small to allow completion of handoff; SUs start to cycle between

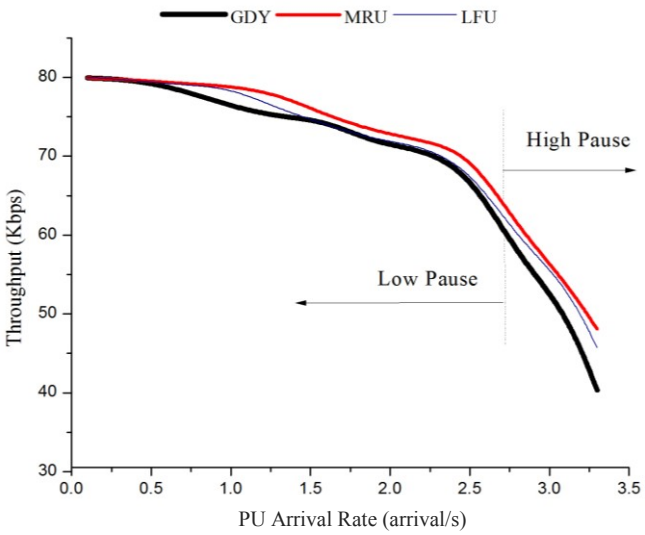

Figure 19. Effect of PU arrival rate on throughput of SU in DHCP-based MIPv6

pause and channel sensing phases (Fig. 2); so there is a gradual degradation of throughput performance (Fig. 19). Comparatively, DHCP-based MIPv6 performs better than the other two versions do, implying that the former could be a better choice in CRNs.

Now, we focus our attention to the selection strategies (different colors in Figs. 18 and 19 indicate them). Fig. 18 shows that, for $\lambda_p\leq2.2$, the MRU strategy performs better than LFU and GDY strategies. This is because the MRU strategy always finds those free channels, which can be used for a longer period of time without needing to perform another IP handoff shortly. That is not true for the other two strategies. However, when $\lambda_p>2.2$, the average spectrum hole duration becomes very small and is entirely consumed by the MIPv6 handoff procedure in all the three spectrum selection strategies. So, all three performs equally bad then. Since MRU always selects the longest spectrum hole, it wastes more time than other two strategies in RA-based MIPv6 (Fig. 18). However, in case of DHCP-based MIPv6, wastage of spectrum hole due to MIPv6 handoff operation is reduced. Hence, MRU strategy performs better than LFU and GDY do (Fig. 19).

For $0.1\leq E[X_p]\leq0.4$, the number of IP handoffs is increasing. In particular, for $0.1\leq E[X_p]\leq0.3$, all IP handoffs are completed successfully, leading to minor throughput degradation largely due to lengthy MIPv6 handoff operation only (Fig. 20). But, for $0.3<E[X_p]\leq0.4$, most of the IP handoffs are incomplete. As a result, the throughput of the SUs drops quickly (Fig. 21). Also, when $E[X_p]>0.4$, the number of IP handoffs itself is reduced because the SUs are mostly cycling between channel sensing and pause phases (Fig. 2). As a result, the throughput of the SUs degrades sharply (Fig. 20). In DHCP-based MIPv6, for $E[X_p]<0.4$, all IP handoffs are successfully completed due to elimination of T_{DAD}. But, for $E[X_p]>0.4$, the SUs are unable to find spectrum holes and cycles between channel sensing and

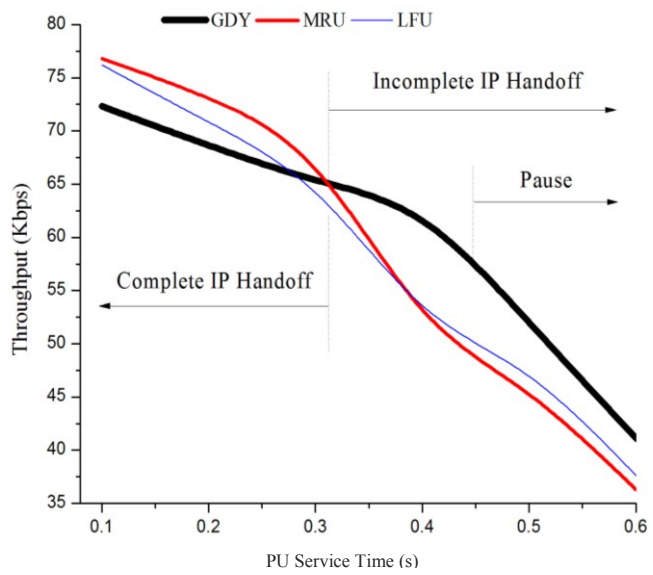

Figure 20. Impact of PU service time on throughput of SU in case of RA-based MIPv6

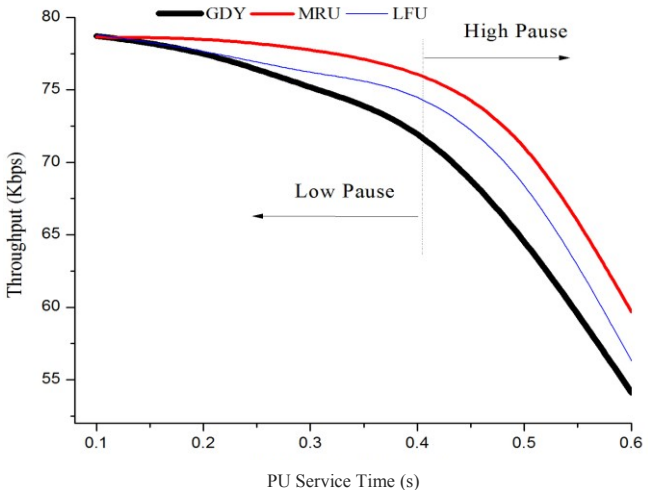

Figure 21. Impact of PU service time on throughput of SU in DHCP-based MIPv6

pause phases, and hence, there is a sharp degradation of throughput in this region (Fig. 21).

VI. Conclusion And Future Work

We have analyzed the number of IP handoffs resulting from spectrum mobility in the absence of spatial mobility. Our study has carried out a root-cause analysis of the observation that MIPv6 cannot work properly in CRNs, and reveals that it is due to high values of RA interval, lifetime period of CoA, and DAD period. That is why the performance of MIPv6 degrades considerably especially when the spectrum holes are becoming smaller with more PUs turning active at a higher rate. So, our first recommendation is that the values for these parameters must be reduced to appropriate levels for possible use of MIPv6 in CRNs.

Our second conclusion is that, for lower values of PU traffic parameters, MRU and LFU have better performance than GDY has; but, for higher values of those parameters, GDY is better than MRU and LFU. Our future work includes design a dynamic spectrum selection strategy to fit with MIPv6 for heterogeneous spectrum mobility scenarios in CRNs in order to improve the throughput of SUs further.

References

[1] M. K. Rana, B. Sardar, S. Mandal, and D. Saha, "Analyzing the Effect of Spectrum Mobility on Mobile IPv6 in Cognitive Radio Networks," The Sixth International Conference on Advances in Cognitive Radio (COCORA 2016), IARIA, February 2016, pp. 26-32, ISSN: 2308-4251, ISBN: 978-1-61208-456-5.

[2] B. Al-Mubarak, "WiFi for UAE Mobile Service Providers: Offloading Mobile Data Traffic to Wi-Fi Can Save UAE Operators up to US$316 Million," Cisco Internet Business Solutions Group (IBSG), Cisco, January 2013.

[3] K. Patil, R. Prasad, and K. Skouby, "A Survey of Worldwide Spectrum Occupancy Measurement Campaigns for Cognitive Radio," Devices and Communications (ICDeCom), International Conference on, Mesra, 2011, pp. 1-5, doi: 10.1109/ICDECOM.2011.5738472.

[4] S. Buljore, H. Harada, S. Filin, and V. Ivanov, "Architecture and Enablers for optimized Radio Resource Usage in Heterogeneous Wireless Access Networks: The IEEE 1900.4 working group," IEEE Communications Magazine, vol. 47, no. 1, pp. 122-129, January 2009.

[5] ETSI - European Telecommunications Standards Institute, Retrieved from http://www.etsi.org/, July 2016.

[6] ITU-R, RadioCommunication sector of ITU, "Introduction of CR systems in the Wireless World-Research Achievements and Future Challenges for End-to-End Efficiency," Report ITU-R M.2330-0, November 2014.

[7] I. Christian, S. Moh, I. Chung, and J. Lee, "Spectrum mobility in cognitive radio networks," IEEE Communications Magazine, vol. 50, June 2012, pp. 114 – 121.

[8] G. Wu, M. Mizuno, and P. J.M. Havinga, "MIRAI architecture for heterogeneous network," IEEE Communications Magazine, vol. 40, no. 2, February 2002, pp. 126-134, doi=http://dx.doi.org/10.1109/35.983919.

[9] C. Perkins, D. Johnson, and J. Arkko, "Mobility support in IPv6," RFC 6275, IETF, 2011.

[10] M. Kataoka, T. Ishikawa, S. Hanaoka, M. Yano, and S. Nishimura, "Evaluation of inter base station handover for cognitive radio," Proceeding on IEEE Radio and Wireless Symposium, January 2008, pp. 251-254.

[11] Y. S. Chen and J. S. Hong, "A Relay-Assisted Protocol for Spectrum Mobility and Handover in Cognitive LTE Networks," in IEEE Systems Journal, vol. 7, no. 1, pp. 77-91, March 2013.

[12] J. F. Weng, B. H. Ku, J. C. Chen, and W. T. Chen, "Channel holding time of packet sessions in all-IP cellular networks", Proc. IEEE ICPADS, December 2014, pp. 404-411.

[13] M. Hoyhtya, J. Lehtomaki, J. Kokkoniemi, M. Matinmikko, and A. Mammela, "Measurements and analysis of spectrum occupancy with several bandwidths," IEEE International Conference on Communications (ICC, 2013), Budapest, 2013, pp. 4682-4686, doi: 10.1109/ICC.2013.6655311.

[14] J. Seob Lee, S. J. Koh, and S. H. Kim, "Analysis of handoff delay for Mobile IPv6," Vehicular Technology Conference (VTC2004), IEEE 60th, Vol. 4, 2004, pp. 2967-2969.

[15] R. Droms, J. Bound, T. Lemon, C. Perkins, and M. Carney, "Dynamic Host Configuration Protocol for IPv6 (DHCPv6)," RFC 3315, IETF, 2003.

[16] Network simulator (ns), version 3, Retrieved from http://www.nsnam.org/, January 2016.

[17] M. K. Rana, B. Sardar, S. Mandal, and D. Saha, "Implementation and performance evaluation of a mobile IPv6 (MIPv6) simulation model for ns-3," Simulation Modelling Practice and Theory, Volume 72, March 2017, pp. 1-22, ISSN 1569-190X, http://dx.doi.org/10.1016/j.simpat.2016.12.005.

[18] L. C. Wang, C. W. Wang, and C. J. Chang, "Optimal target channel sequence for multiple spectrum handoffs in cognitive radio networks," IEEE Transactions on Communication," vol. 60, September 2012, pp. 2444-2455.

[19] L.-C. Wang, C.-W. Wang, and C.-J. Chang, "Modeling and Analysis for Spectrum Handoffs in Cognitive Radio Networks," IEEE Transactions on Mobile Computing," vol. 11, July 2012, pp. 1499-1513.

[20] R. Southwell, J. Huang, and X. Liu, "Spectrum mobility games," INFOCOM, 2012 Proceedings IEEE, March 2012, pp. 37-45.

[21] J. Sztrik, "Basic queueing theory," University of Debrecen, Faculty of Informatics, 2011.

[22] C. W. Wang, L. C. Wang, and Adachi F., "Modeling and Analysis for Reactive-Decision Spectrum Handoff in Cognitive Radio Networks," Proceedings IEEE Global Telecommunications Conference (GLOBECOM 2010), December 2010, pp. 1-6.

[23] S. U. Yoon, and E. Ekici, "Voluntary Spectrum Handoff: A Novel Approach to Spectrum Management in CRNs," IEEE International Conference on Communications (ICC), May 2010, pp. 1-5, 23-27.

[24] G. Yuan, R. C. G.rammenos, Y. Yang, and W. Wang, "Performance Analysis of Selective Opportunistic Spectrum Access With Traffic Prediction," IEEE Transactions on Vehicular Technology, vol. 59, no. 4, May 2010, pp. 1949-1959.

[25] ETSI, "Universal Mobile Telecommunications System (UMTS): Selection Procedures for the Choice of Radio Transmission Technologies of the UMTS," Technical Report UMTS 30.03, version 3.2.0, April 1998.

[26] Y. H. Han, and S. H. Hwang, "Movement detection analysis in mobile IPv6," IEEE Communications Letters, January, 2006, pp. 59-61, doi: 10.1109/LCOMM.2006.1576570.